

**Microwave frequency combs through the rotational enhanced magnetostrictive effect**Qin Wu,<sup>1,2,\*</sup> Hao-Jin Sun,<sup>3</sup> Yu-Dong Chen,<sup>1</sup> and Zeng-Xing Liu<sup>3</sup><sup>1</sup>*The First Dongguan Affiliated Hospital, Guangdong Medical University, Dongguan, Guangdong 523808, China*<sup>2</sup>*School of Biomedical Engineering, Guangdong Medical University, Dongguan, Guangdong 523808, China*<sup>3</sup>*School of Electronic Engineering & Intelligentization, Dongguan University of Technology, Dongguan, Guangdong 523808, China*

(Received 27 February 2024; revised 6 May 2024; accepted 22 May 2024; published 5 August 2024)

Microwave frequency combs have attracted particular attention due to their great application prospects in microwave communication and measurement. In recent years, the scheme of generating microwave frequency combs based on an optical method has been widely concerned; however, the investigation of obtaining microwave frequency combs based on a magnetic method has rarely been reported. Here, an efficient mechanism for the generation of microwave frequency combs induced by the rotational enhanced magnetostrictive effect is theoretically proposed. The results show that the magnetostrictive interaction can be greatly enhanced by introducing the Sagnac effect, and then a robust microwave frequency comb can be observed even at low power. Furthermore, when we change the incidence direction of the driving field, the generation of microwave frequency combs has strong nonreciprocity. Our propose thus provides a pathway for the generation of a flat microwave frequency comb based on magnonic platforms that may be beneficial for microwave frequency metrology and spectroscopy, as well as an in-depth understanding of magnomechanical nonlinearity.

DOI: [10.1103/PhysRevA.110.023507](https://doi.org/10.1103/PhysRevA.110.023507)**I. INTRODUCTION**

Microwave frequency combs, the analog of optical frequency combs generated in the microwave (gigahertz) frequency range, have the advantages of large number of spectral lines, wide frequency range, and high accuracy of spectral line spacing, and they have important applications in communication, sensing, and other fields [1–5]. At present, the main generation methods of microwave frequency combs are based on electrical and photoelectric methods, for example, microwave-frequency-comb generation utilizing a semiconductor laser subject to optical pulse [3], optical generation of a precise microwave frequency comb by harmonic frequency locking [4], and so on [5]. Furthermore, the generation of microwave frequency combs as a result of a  $\chi^{(3)}$  nonlinearity in a high  $Q$ -factor sapphire whispering gallery mode resonator introduced by a dilute concentration of paramagnetic  $\text{Fe}^{3+}$  spins has also been studied [6,7]. The use of magnetics to generate microwave frequency combs, compared to the previous scheme, has inherent advantages in, for instance, ultranarrow line-wide comb teeth and being highly tunable through external magnetic fields. Whereas, the weak spin interaction has been a major bottleneck for generating robust microwave frequency combs.

The Sagnac effect, first proposed by Sagnac in 1913, refers to the interesting phenomenon that interference fringes on a ring interferometer screen will move when the toroidal plane has rotational angular velocity [8,9]. Over the past decades, the research of combining the Sagnac effect with an optical microcavity has attracted more and more attention

[10–19]. In particular, the rotation-induced Sagnac frequency shift leads to many exotic physical phenomena, such as rotating optical microcavities with broken chiral symmetry [12], irreversible refraction generation in spinning resonators [13], the exceptional-point-enhanced Sagnac effect [14], nonreciprocal photon blockade [16], and so on [17–19]. In recent years, a fundamentally different type of spin wave–mechanical oscillator interaction has attracted a lot of attention, which is the magnetostrictive coupling between magnons and mechanical motion studied in magnomechanical systems [20–37]. Inspired by these works, the concept of a spinning microwave magnomechanical system has been theoretically introduced, where an yttrium iron garnet (YIG) sphere supporting both the magnon and the phonon modes is coupled to a spinning resonator [38–45]. Many intriguing phenomena have been reported in the spinning magnomechanical system, ranging from nonreciprocal transmission and magnon-phonon entanglement [38] to nonreciprocal phonon laser [39] to nonreciprocal two-color second-order sideband generation [40,41] and nonreciprocal quantum coherence in spinning magnomechanical systems [42].

In the present work, we present an efficient mechanism for the generation of microwave frequency combs through the rotational enhanced magnetostrictive effect in a spinning magnomechanical system. The results indicate that the Sagnac effect induced by a rotational microwave resonator has a positive response to the nonlinear magnetostrictive interaction and then promotes the generation of microwave frequency combs. Numerical calculations of the magnomechanical dynamics show that, even under a weak microwave drive, a robust microwave frequency comb can be observed in the output spectrum, which can be effectively controlled by adjusting the rotation speed. More importantly, just by changing

\*wuqin@gdmu.edu.cn

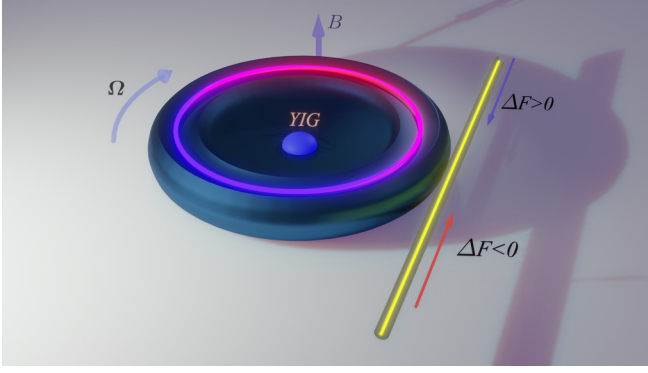


FIG. 1. Schematic diagram of the rotatable cavity magnomechanical system consisting of a spinning microwave resonator with the angular velocity  $\Omega$  and a YIG sphere placed at the maximum of the magnetic field. A microwave driving field enters the spinning microwave resonator causing the microwaves circulating in the resonator to experience a Sagnac-Fizeau shift,  $\Delta_F$ . When the driving field input is from the right side (blue arrow), the Fizeau shift  $\Delta_F > 0$ , and when the driving field input is from the left side (red arrow), the Fizeau shift  $\Delta_F < 0$ .

the incidence direction of the driving field, the generation of comb teeth is no longer observed in the output spectrum. This suggests that the rotation-induced microwave frequency comb is nonreciprocal, which reminds us of the possibility that the generation of microwave frequency combs can be highly tuned by the rotation speed and direction of the resonator. In addition to the fundamental scientific significance, our results broaden the regime of cavity magnomechanics and may provide applications for achieving nonreciprocal microwave frequency combs based on magnonic platforms [46–48].

## II. PHYSICAL MODEL AND THEORY

A schematic diagram of the rotational cavity magnomechanical system, as shown in Fig. 1, consisting of a spinning microwave resonator that supports the whispering gallery mode and a YIG sphere placed at the maximum of the magnetic field [39]. The microwave driving field coupled with the spinning microwave resonator excites the ferromagnetic Kittel mode (i.e., the magnonic mode) of the YIG sphere. The external magnetic field with the strength  $B$  is applied to the YIG sphere to saturate the magnetization and establish the coherent coupling between the Kittel mode and the microwave resonator mode. The frequency of the ferromagnetic Kittel mode  $\omega_m$  can be dynamically regulated by adjusting the strength of the external magnetic field, i.e.,  $\omega_m = \gamma B$  with the gyromagnetic ratio  $\gamma/2\pi = 28$  GHz/T [49]. Furthermore, under the action of the external magnetic field, the different magnetization caused by the excitation of the Kittel mode will induce the deformation of the YIG sphere. In the meantime, the deformation of the YIG sphere in response to the external magnetic field will also affect the magnetization, giving rise to interactions between the Kittel mode and the deformation mode (the so-call magnetostriction effect) [20,21,23,24]. Assume that the microwave resonator is pumped by a two-tone microwave driving field with the driving amplitude  $\xi_j = \sqrt{P_j/\hbar\omega_j}$  ( $j = l$  and  $p$ ), where  $P_j$

is the power of the microwave driving field and  $\omega_j$  is the corresponding drive frequency. For ease of description, the two-tone microwave drive field is referred to as the microwave pumping field and the probe field, although the power of the microwave probe field may exceed that of the pumping field. According to the Sagnac effect, for a microwave resonator rotating at angular velocity  $\Omega$ , the resonant frequency of the microwave resonator will change, i.e., the microwave circulating in the resonator undergoes a Sagnac-Fizeau shift [13],  $\omega'_a = \omega_a + \Delta_F$ , with

$$\Delta_F = \pm\omega_a \frac{nr\Omega}{c} \left( 1 - \frac{1}{n^2} - \frac{\lambda}{n} \frac{dn}{d\lambda} \right), \quad (1)$$

where  $\omega_a$  is the resonance frequency for the stationary resonator.  $n$  and  $r$  are the refractive index and the radius of the resonator, respectively.  $c$  and  $\lambda$  are the speed and wavelength of the microwave photon in vacuum, respectively.  $dn/d\lambda$  is the dispersion term characterizing the relativistic origin of the Sagnac effect. When the resonator spinning and the microwave rotation are along the same direction, i.e., the microwave driving field is incident from the right side (blue arrow in Fig. 1), a positive Sagnac-Fizeau shift can be obtained,  $\Delta_F > 0$ . Conversely, if the microwave driving field input from the left side (red arrow in Fig. 1), i.e., the resonator spinning and the microwave rotation are in opposite directions, the Sagnac-Fizeau shift is negative,  $\Delta_F < 0$ . In particular, a zero Sagnac-Fizeau shift,  $\Delta_F = 0$ , corresponds to the situation in which the resonator is stationary (i.e.,  $\Omega = 0$ ). Studies have shown that, similar to the incident field pump, cavity rotation has a vital impact on mechanical displacement and intracavity photon amplitude [17,19]. More importantly, the Sagnac-Fizeau shift provides a feasible way to realize the tunable microwave resonant frequency and will be conducive to the resonance between the coupled cavity-magnonic system and other subsystems. It should be noted that the cavity frequency shift can also be achieved in other ways, for example, a tunable cryogenic microwave cavity based on a double-stub re-entrant cavity has been experimentally realized. The cavity frequency can be tuned *in situ* by up to 1.5 GHz, approximately 15% of its original resonance frequency (10 GHz), and moreover, the system maintains an approximately constant quality factor [50].

Considering the Sagnac-Fizeau shift, the Hamiltonian of the rotatable cavity magnomechanical system can be written as [39]

$$\begin{aligned} H = & \hbar\omega'_a \hat{a}^\dagger \hat{a} + \hbar\omega_m \hat{m}^\dagger \hat{m} + \hbar\omega_b \hat{b}^\dagger \hat{b} \\ & + \hbar g_{ma} (\hat{a} \hat{m}^\dagger + \hat{a}^\dagger \hat{m}) + g_{mb} \hat{m}^\dagger \hat{m} (\hat{b}^\dagger + \hat{b}) \\ & + i\hbar\sqrt{2k_a} (\xi_l \hat{a}^\dagger e^{-i\omega_l t} + \xi_p \hat{a}^\dagger e^{-i\omega_p t} - \text{H.c.}), \quad (2) \end{aligned}$$

where  $\hbar$  is the reduced Planck's constant and  $\hat{a}(\hat{a}^\dagger)$  is the boson annihilation (creation) operator of the microwave cavity mode.  $\hat{m} = \sqrt{\frac{V_m}{2\hbar e M}} (M_x - iM_y)$  is the annihilation operator of the Kittel mode, with  $V_m$  being the YIG sphere volume,  $M$  the saturation magnetization, and  $M_{x,y,z}$  the magnetization components [20].  $\hat{b}(\hat{b}^\dagger)$  is the annihilation (creation) operator of the deformation mode with the frequency  $\omega_b$ . The cavity photon and the magnonic mode are coupled with each other by magnetic dipole interaction, and the coupling strength is

$g_{ma}$ . Furthermore, the coupling between the magnonic and vibrational modes through magnetostrictive effect can be described by a radiation pressurelike Hamiltonian [51], i.e.,  $H_{\text{int}} = g_{mb}\hat{m}^\dagger\hat{m}(\hat{b}^\dagger + \hat{b})$ , with the coupling strength  $g_{mb}$ .  $\kappa_a$  refers to the decay rate of the microwave cavity mode and H.c. is the Hermitian conjugate. In order to make the driving terms time independent, a rotating frame at the microwave driving frequency  $\omega_l$  is adopted, i.e., applying the unitary transformation  $\mathbf{U}(t) = \exp(-i\omega_l\hat{a}^\dagger\hat{a}t - i\omega_l\hat{m}^\dagger\hat{m}t)$ . Therefore, the Hamiltonian of the system can be rewritten as

$$\begin{aligned} H &= \mathbf{U}(t)H\mathbf{U}^\dagger(t) - i\hbar\mathbf{U}(t)\frac{\partial\mathbf{U}^\dagger(t)}{\partial t} \\ &= \hbar\Delta'_a\hat{a}^\dagger\hat{a} - \hbar\Delta_m\hat{m}^\dagger\hat{m} + \hbar\omega_b\hat{b}^\dagger\hat{b} \\ &\quad + \hbar g_{ma}(\hat{a}\hat{m}^\dagger + \hat{a}^\dagger\hat{m}) + \hbar g_{mb}\hat{m}^\dagger\hat{m}(\hat{b}^\dagger + \hat{b}) \\ &\quad + i\hbar\sqrt{2\kappa_a}(\xi_l\hat{a}^\dagger + \xi_p\hat{a}^\dagger e^{-i\Delta_p t} - \text{H.c.}), \end{aligned} \quad (3)$$

where  $\Delta'_a = \Delta_F - \Delta_a$ , with  $\Delta_a = \omega_l - \omega_a$  being the detuning between the microwave cavity mode and the driving field frequency.  $\Delta_m = \omega_l - \omega_m$  is the detuning between the magnonic mode and the driving field frequency and  $\Delta_p = \omega_p - \omega_l$  is the beat frequency between the driving field and the probe field. The evolution of the rotatable cavity magnomechanical system can be described by the Heisenberg-Langevin equations, i.e.,  $\dot{\hat{o}} = i/\hbar[H, \hat{o}] + \hat{\sigma}$  ( $\hat{o} = \hat{a}, \hat{b}, \hat{m}$ ); hence, we can obtain the following coupled equations:

$$\begin{aligned} \dot{a} &= (i\Delta_a - i\Delta_F - \kappa_a)a - ig_{ma}m + \sqrt{2\kappa_a}(\xi_l + \xi_p e^{-i\Delta_p t}), \\ \dot{b} &= (-i\omega_b - \kappa_b)b - ig_{mb}m^\dagger, \\ \dot{m} &= (i\Delta_m - \kappa_m)m - ig_{ma}a - ig_{mb}m(b^\dagger + b), \end{aligned} \quad (4)$$

where  $\kappa_j$  ( $j = b, m$ ) is the damping rate of the vibrational mode and the magnonic mode, respectively. Here, in the semiclassical approximation, all the operators are reduced to their expectation values, viz.,  $o(t) = \langle \hat{o}(t) \rangle$ . Moreover, the mean-field approximation by factorizing averages is also used, and the quantum noise terms are dropped safely [52]. Equations (4) are the nonlinear partial differential equations, and the nonlinearity of the system is derived from the magnetostrictive interaction between the magnonic mode and the vibrational mode. The output field from the cavity magnomechanical system can be obtained by using the input-output relation [38]  $a_{\text{out}}(t) = a_{\text{in}}(t) - \sqrt{2\kappa_a}a(t)$ , where  $a_{\text{in}}(t) = \xi_l + \xi_p e^{-i\Delta_p t}$  is the effective microwave input field in a rotating frame at  $\omega_l$ . The time evolution of the output field can be obtained by solving the Eqs. (4), and the output spectrum of the system can be obtained by doing the fast Fourier transform of the time series, i.e.,  $S(\omega) \propto \int_{-\infty}^{\infty} a_{\text{out}}(t)e^{-i\omega t} dt$ . In the present work, Eqs. (4) are solved numerically by using the Runge-Kutta method, and for convenience, the initial conditions are chosen as  $a|_{t=0} = 0$ ,  $b|_{t=0} = 0$ , and  $m|_{t=0} = 0$ .

### III. DISCUSSION

The microwave frequency comb spectra output from the cavity magnomechanical system with and without the Sagnac-Fizeau shift are plotted in Fig. 2. Obviously, it is difficult to generate a robust microwave frequency comb spectrum in the absence of the Sagnac effect, i.e.,  $\Delta_F/\omega_b = 0$ , which

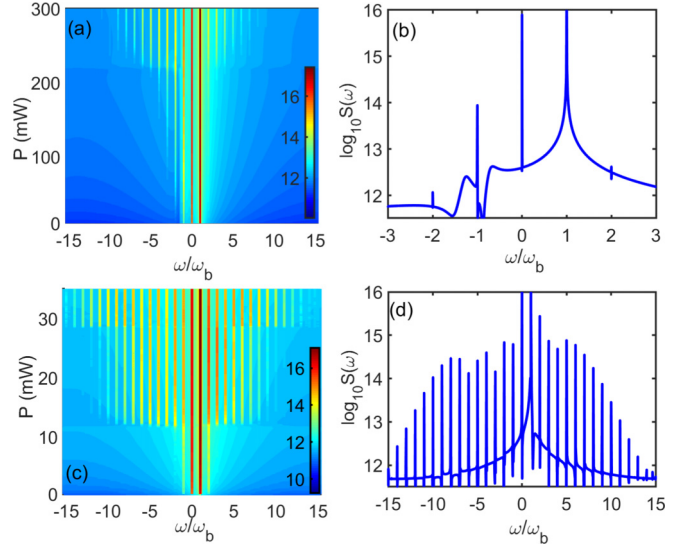


FIG. 2. Microwave frequency comb spectra output from the rotatable cavity magnomechanical system are shown vary with the power of the microwave driving field in the case of (a) without the Fizeau shift ( $\Delta_F = 0$ ) and (c) in the presence of the Fizeau shift ( $\Delta_F \neq 0$ ). The color indicates the amplitude of the combs. In the case of  $\Delta_F = 0$ , the microwave frequency comb spectrum is plotted in panel (b) under the microwave pumping powers  $P_l = 30$  mW. Under the same microwave pumping power, the comb spectrum is shown in (d) in the case of  $\Delta_F/\omega_b = 2$ . Here, a set of experimentally feasible values are used [20]:  $\omega_a/2\pi = 7.86$  GHz,  $\omega_b/2\pi = 11.42$  MHz,  $2\kappa_a/2\pi = 3.35$  MHz,  $2\kappa_m/2\pi = 1.12$  MHz,  $2\kappa_b/2\pi = 300$  Hz,  $g_{ma}/2\pi = 3.2$  MHz,  $g_{mb}/2\pi = 9.88$  mHz,  $\Delta_a = \Delta_m = \Delta_p = \omega_b$ , and  $\xi_p = 10\xi_l$ .

means that weak nonlinear magnetostriction interactions pose challenges for the generation of microwave frequency combs. Specifically, a significant microwave frequency comb generation is observed in the output spectrum only when the power of the microwave drive field exceeds 200 mW, as shown in Fig. 2(a). To take one example, when the driving field power is relatively weak,  $P_l = 30$  mW, as shown in Fig. 2(a), only a few sideband combs can be observed in the output spectrum, and the comb intensity is very weak. In this case, the frequency spectrum can be regarded as a perturbation spectrum, that is, the higher the order of the comb tooth considered, the smaller the amplitude obtained. Furthermore, it should be pointed out that the output spectrum has been shifted by a microwave input field frequency  $\omega_l$  as a whole, because the coupled Eqs. (4) describe the evolution of the optical field in a frame rotating at frequency  $\omega_l$ . Intriguingly, when the Sagnac effect was considered ( $\Delta_F/\omega_b = 2$ ), as shown in Fig. 2(c), the threshold power of microwave frequency comb generation is drastically reduced to about  $P_{\text{th}} \approx 12$  mW under the same parameter conditions, which is about 20 times less than the case without the Fizeau shift. More specifically, we can see that a robust ultra-wideband microwave frequency comb spectrum can be obtained under a weaker driving field, indicating that the magnetostrictive nonlinearity is greatly enhanced by the Sagnac effect. By the same example, when the driving field power  $P_l = 30$  mW, as shown in Fig. 2(d), about 30 sideband comb teeth appear in the output spectrum, and the

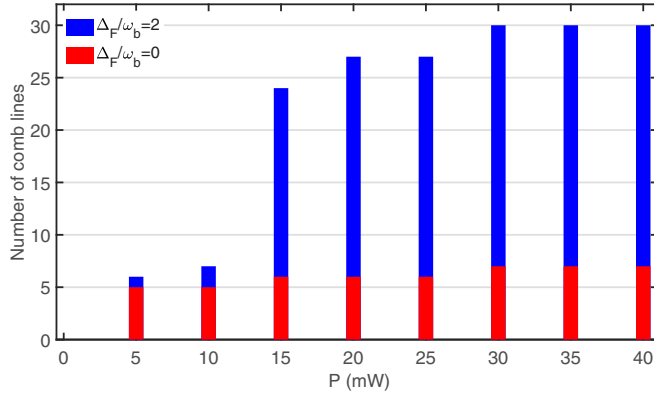


FIG. 3. Number of comb lines under the different microwave drive field powers in the presence of the Sagnac-Fizeau shift  $\Delta_F/\omega_b = 2$  (blue columns) and in the absence of the Sagnac-Fizeau shift  $\Delta_F/\omega_b = 0$  (red columns). The other parameters are the same as those in Fig. 2.

strength of each comb is significantly enhanced. In addition, we can observe a typical nonperturbed signal [53,54]. For example, there is a plateau region in the output spectrum where all combs have almost the same intensity, and where the fifth-order comb strength is greater than the fourth-order comb strength.

Further, in order to visually reflect the high dependence of microwave frequency comb generation on the Sagnac effect, the comparison of the number of comb lines under the same driving field power is shown in Fig. 3. In the absence of the Sagnac effect, as the red columns show in Fig. 3, the number of comb lines is almost unchanged when the microwave incident field power increases from  $P_l = 5$  mW to  $P_l = 40$  mW. However, when the Sagnac-Fizeau shift was considered, as the blue columns show, a significant increase in the number of comb lines is observed with the same microwave drive field power. Since a small microwave drive power (e.g.,  $P_l = 15$  mW) is sufficient to produce a robust microwave frequency comb, our proposal thus provides a pathway for the generation of a flat magnonic frequency comb under a low-power driving condition.

Physically, the generation of microwave frequency combs is essentially a process in which nonlinear magnomechanical interactions lead to the production and absorption of multiple phonons, which is similar to the physical mechanism of the generation of high-order harmonics induced by nonlinear interactions between light and atoms (i.e., the production and absorption of multiple photons) [55–57]. More specifically, the phonon can couple with the microwave photon through frequency up-conversion and down-conversion processes and excite the sum-frequency ( $\omega_l + \omega_b$ ) and difference-frequency ( $\omega_l - \omega_b$ ) modes, while these excitation modes can further couple with the phonon mode to generate higher-order frequency modes. Consequently, a series of equally spaced teeth around the pumped mode, i.e.,  $\omega_l \pm j\omega_b$ , with  $j$  being the order of the comb teeth, will appear in the output spectrum, which is the main characteristic of the frequency combs [58,59]. Therefore, the study of microwave frequency combs through the nonlinear magnetostrictive interaction is of great

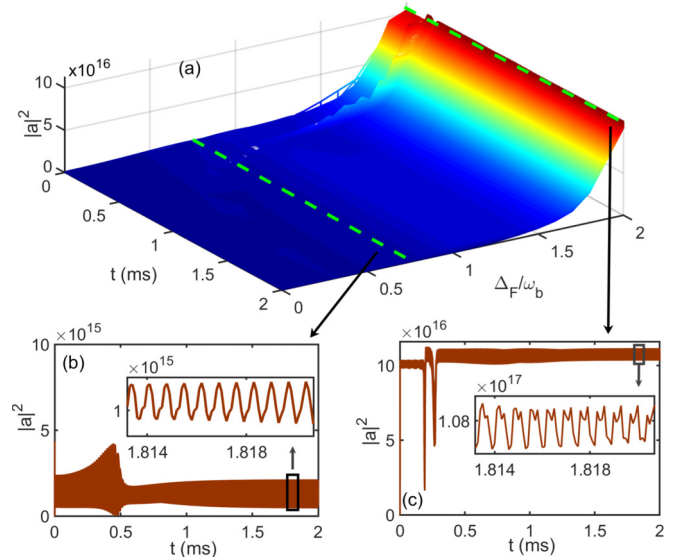


FIG. 4. Dependence of the microwave photon number output from the cavity magnomechanical system on the Sagnac-Fizeau shift  $\Delta_F/\omega_b$ . (a) The surface plot of the microwave photon number evolution. Evolution of system dynamics under different Fizeau shifts: (b)  $\Delta_F/\omega_b = 0.7$  and (c)  $\Delta_F/\omega_b = 2$ , respectively. The microwave driving field power  $P_l = 30$  mW and the other parameters are the same as those in Fig. 2.

significance for a deeper understanding of magnomechanical nonlinearity and their related applications.

In what follows, to investigate the influence of the Sagnac effect on the evolution of magnomechanical dynamics, the dependence of the evolution of the microwave photon number on the Sagnac-Fizeau shift  $\Delta_F/\omega_b$  is shown in Fig. 4(a). We can see that the microwave photon number increases rapidly as the Fizeau shift changes, reaching a maximum at  $\Delta_F/\omega_b \approx 2$ . To be specific, when the Fizeau shift  $\Delta_F/\omega_b = 0.7$ , the dynamic evolution of the system undergoes a process where the microwave photon number grows rapidly over time, then decreases rapidly to  $|a|^2 \sim 10^{15}$ , and finally stabilizes at this magnitude, as shown in Fig. 4(b). When we increase the Fizeau shift to  $\Delta_F/\omega_b = 2$ , as shown in Fig. 4(c), the system undergoes a rapid oscillation before reaching stability, at which point the microwave photon number  $|a|^2 \sim 10^{17}$ , an increase of 2 orders of magnitude over the case of  $\Delta_F/\omega_b = 0.7$ . This indicates that the enhancement of the system nonlinearity caused by the Sagnac effect has a significant effect on the increase of the microwave photon number, and thus, the generation of microwave frequency combs is greatly enhanced.

Nonreciprocity refers to the fact that when the symmetry of a system is broken, the behavior or effect observed in one direction is different from that observed in the opposite direction, which is important for a range of applications [60–62]. Many interesting nonreciprocal phenomena induced by the Fizeau light-dragging effect have been extensively investigated and have progressed enormously in recent years [38–45]. A natural question is whether nonreciprocal microwave frequency combs can be achieved based on the rotatable cavity magnomechanical system. For this purpose,

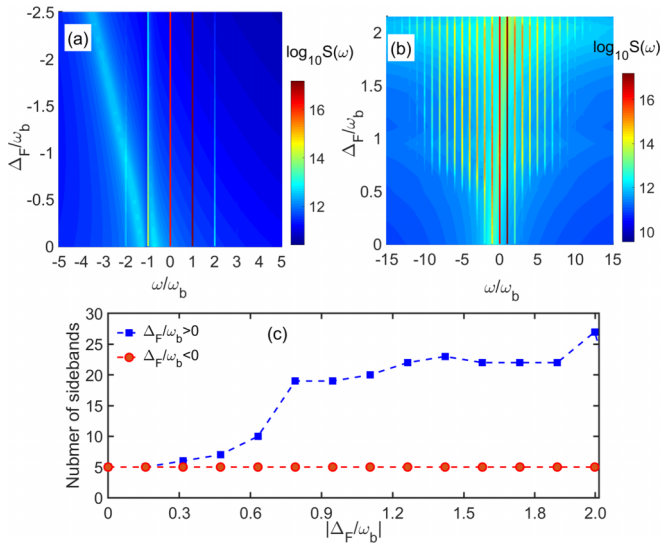


FIG. 5. Microwave frequency comb spectra vary with the Sagnac-Fizeau shift  $\Delta_F/\omega_b$  under different microwave incidence directions: (a)  $\Delta_F/\omega_b < 0$  and (b)  $\Delta_F/\omega_b > 0$ . (c) Number of sideband combs as a function of the Sagnac-Fizeau shift  $\Delta_F/\omega_b$  in the case of  $\Delta_F/\omega_b < 0$  (red dots) and  $\Delta_F/\omega_b > 0$  (blue squares). For convenience, take the absolute value of  $\Delta_F/\omega_b$ . The microwave driving-field power  $P_l = 30$  mW. The other parameters are the same as those in Fig. 2.

we change the incidence direction of the driving field; i.e., the resonator spinning and the microwave rotation are in opposite directions (the Sagnac-Fizeau shift  $\Delta_F < 0$ ). Interestingly, we find that the generation of microwave frequency combs has strong nonreciprocity. Namely, by controlling the incidence direction of the driving field, the microwave frequency comb is allowed to be generated from one side, but the other side is suppressed. Physically, the nonreciprocal behavior of the comb generation can be understood from the transmission of the system. When the microwave input field comes from different directions, the transmission in the rotating resonator system is identical, except for the sign of  $\Delta_F$  [13]. The rotating system resonantly absorbs the microwave input field entering from one side, while off-resonantly transmitting the counterpropagating microwave driving field, thus achieving nonreciprocal comb generation. As shown in Fig. 5, the generation of microwave frequency combs varies with the Sagnac-Fizeau shift  $\Delta_F/\omega_b$  under different microwave incidence directions showing completely different results. To be specific, if the input field is incident on the resonator from the left side, i.e.,  $\Delta_F < 0$ , as shown in Fig. 5(a), then only a few combs appear in the output spectrum. Even if the rotational angular velocity increases, there is no significant change to the combs' number. For comparison, the case of the input field entering the resonator from right side, i.e.,  $\Delta_F > 0$ , is also discussed. A high dependence of the microwave frequency comb generation on the Fizeau shift is observed and a more clear result is shown in Fig. 5(b) with the same experimental parameters [20]. We can see that the generation of microwave frequency combs is greatly enhanced with the increase of the resonator rotation speed, and ultimately, a robust microwave frequency comb is achieved near  $\Delta_F/\omega_b \sim 2$ , which is

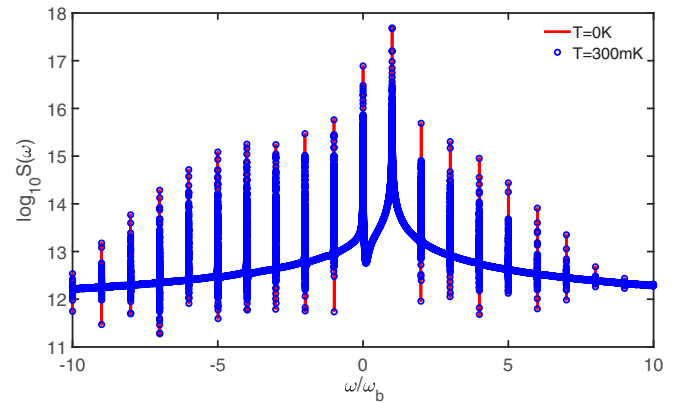


FIG. 6. The microwave frequency comb spectra under different temperatures  $T = 0$  K and  $T = 300$  K, respectively. The Sagnac-Fizeau shift  $\Delta_F/\omega_b = 1$  and the microwave driving field power  $P_l = 30$  mW. The other parameters are the same as those in Fig. 2.

consistent with the result that the number of microwave photons varies with the Sagnac-Fizeau shift shown in Fig. 4(a). In addition, number of sideband combs as a function of the Sagnac-Fizeau shift  $\Delta_F/\omega_b$  under different microwave incidence directions is shown in Fig. 4(c). Obviously, when the input field is incident on the resonator from the right side (blue squares), a robust microwave frequency comb can be obtained, which is significantly better than when the drive field is incident on the other side (red dot). These results show that the generation of microwave frequency combs induced by the rotational enhanced magnetostrictive effect has strong nonreciprocity, which provides a new method for the regulation of microwave frequency comb generation and may find applications in one-way amplifiers based on magnonic devices [63,64].

Finally, it is necessary to evaluate the feasibility of microwave frequency combs in experiment. First, we discuss the influence of thermal noise on the generation of magnonic frequency combs. We assume that the system is coupled to a high-temperature thermal bath, namely, the cavity photon mode, the magnonic mode, and the vibrational mode are driven by the thermal noise. Phenomenologically, we add the thermal noise to Eqs. (4), and then the equations are solved numerically with the same experimental parameters. Here, the thermal noises are regarded as Gaussian random numbers with average values  $n_{\text{th}} = (e^{\hbar\omega_o/K_B T} - 1)^{-1}$  [52], where  $o = a, b$ , and  $m$  for the cavity photon mode, the magnonic mode, and the phonon mode, respectively.  $K_B$  is the Boltzmann constant and  $T$  is the ambient temperature. The microwave frequency comb spectrum under room temperature ( $T = 300$  K) is shown in Fig. 6, which, obviously, exhibits almost no difference from the zero-temperature spectrum ( $T = 0$  K). Thus, the generation of microwave frequency combs based on the rotational enhanced magnetostrictive effect is robust against the thermal noise. Second, the Sagnac-Fizeau shift  $\Delta_F$  is proportional to the refractive index, the radius, and the spinning speed of the resonator, i.e.,  $\Delta_F \propto n, r, \Omega$ , as shown in Eq. (1). We consider a dielectric resonator with the high refractive index  $n = 2.2$  and the radius  $r = 6$  cm for estimation. The Sagnac-Fizeau shift  $\Delta_F/\omega_b = 1$  corresponds to the spinning

speed of the resonator,  $\Omega \sim 4$  MHz [13]. Furthermore, a smaller Sagnac-Fizeau shift (e.g.,  $\Delta_F/\omega_b \sim 0.5$ ) is sufficient to induce the generation of microwave frequency combs and introduce a pronounced nonreciprocity, as shown in Fig. 5. Although such rotational speed is experimentally challenging, with continual technological improvements in the rotation and manipulation of spherical dielectrics, it is possible to achieve a resonator with much higher spinning speed [65–68]; therefore, our scheme is expected to be confirmed in future experiments. Importantly, it is possible to extend the generation of frequency combs to other frequency domains, such as the optical frequency domain, the acoustic frequency domain, and the spin-wave frequency domain, due to the excellent compatibility between magnons and other quasiparticles.

#### IV. CONCLUSION

In short, a mechanism for the generation of microwave frequency combs through the rotational enhanced magnetostrictive effect in a rotatable cavity magnomechanical

system is theoretically proposed. We find that the magnetostrictive interaction can be greatly enhanced by introducing the Sagnac effect and thus induces the generation of a flat microwave frequency comb. The numerical simulation results show that the total comb width of the microwave frequency comb can be extended to about 30 orders by rotating the resonator, which is difficult to achieve by increasing the drive field power. Our scheme, therefore, provides an idea for realizing robust microwave frequency combs through rotating the resonator rather than requiring strong driving field power or coupling interactions. Furthermore, we find that the generation of microwave frequency combs has strong nonreciprocity, which opens up the possibility of using magnonic devices to generate nonreciprocal microwave frequency combs.

#### ACKNOWLEDGMENTS

This work was supported by the National Science Foundation (NSF) of China (Grant No. 12105047) and the Guangdong Basic and Applied Basic Research Foundation (Grant No. 2022A1515010446).

- 
- [1] T. M. Fortier, M. S. Kirchner, F. Quinlan, J. Taylor, J. C. Bergquist, T. Rosenband, N. Lemke, A. Ludlow, Y. Jiang, C. W. Oates, and S. A. Diddams, Generation of ultrastable microwaves via optical frequency division, *Nat. Photonics* **5**, 425 (2011).
- [2] S. B. Papp, K. Beha, P. Del’Haye, F. Quinlan, H. Lee, K. J. Vahala, and S. A. Diddams, Microresonator frequency comb optical clock, *Optica* **1**, 10 (2014).
- [3] S.-C. Chan, G.-Q. Xia, and J.-M. Liu, Optical generation of a precise microwave frequency comb by harmonic frequency locking, *Opt. Lett.* **32**, 1917 (2007).
- [4] Y.-S. Juan and F.-Y. Lin, Microwave-frequency-comb generation utilizing a semiconductor laser subject to optical pulse injection from an optoelectronic feedback laser, *Opt. Lett.* **34**, 1636 (2009).
- [5] L. Fan, G.-Q. Xia, T. Deng, X. Tang, X.-D. Lin, Z.-Y. Gao, and Z.-M. Wu, Generation of tunable and ultra-broadband microwave frequency combs based on a semiconductor laser subject to pulse injection from a current modulated laser, *IEEE Photonics J.* **10**, 1 (2018).
- [6] D. L. Creedon, K. Benmessaï, and M. E. Tobar, Frequency conversion in a high  $Q$ -factor sapphire whispering gallery mode resonator due to paramagnetic nonlinearity, *Phys. Rev. Lett.* **109**, 143902 (2012).
- [7] D. L. Creedon, K. Benmessaï, W. P. Bowen, and M. E. Tobar, Four-wave mixing from  $\text{Fe}^{3+}$  spins in sapphire, *Phys. Rev. Lett.* **108**, 093902 (2012).
- [8] E. J. Post, Sagnac effect, *Rev. Mod. Phys.* **39**, 475 (1967).
- [9] W. W. Chow, J. Gea-Banacloche, L. M. Pedrotti, V. E. Sanders, W. Schleich, and M. O. Scully, The ring laser gyro, *Rev. Mod. Phys.* **57**, 61 (1985).
- [10] S. Franke-Arnold, G. Gibson, R. W. Boyd, and M. J. Padgett, Rotary photon drag enhanced by a slow-light medium, *Science* **333**, 65 (2011).
- [11] M. P. J. Lavery, F. C. Speirits, S. M. Barnett, and M. J. Padgett, Detection of a spinning object using light’s orbital angular momentum, *Science* **341**, 537 (2013).
- [12] R. Sarma, L. Ge, J. Wiersig, and H. Cao, Rotating optical microcavities with broken chiral symmetry, *Phys. Rev. Lett.* **114**, 053903 (2015).
- [13] S. Maayani, R. Dahan, Y. Kligerman, E. Moses, A. U. Hassan, H. Jing, F. Nori, D. N. Christodoulides, and T. Carmon, Flying couplers above spinning resonators generate irreversible refraction, *Nature (London)* **558**, 569 (2018).
- [14] Y.-H. Lai, Y.-K. Lu, M.-G. Suh, Z. Yuan, and K. Vahala, Observation of the exceptional-point-enhanced Sagnac effect, *Nature (London)* **576**, 65 (2019).
- [15] H. Jing, H. Lü, S. K. Özdemir, T. Carmon, and F. Nori, Nanoparticle sensing with a spinning resonator, *Optica* **5**, 1424 (2018).
- [16] R. Huang, A. Miranowicz, J.-Q. Liao, F. Nori, and H. Jing, Nonreciprocal photon blockade, *Phys. Rev. Lett.* **121**, 153601 (2018).
- [17] H. Lü, Y.-J. Jiang, Y.-Z. Wang, and H. Jing, Optomechanically induced transparency in a spinning resonator, *Photonics Res.* **5**, 367 (2017).
- [18] Y. Jiang, S. Maayani, T. Carmon, F. Nori, and H. Jing, Nonreciprocal phonon laser, *Phys. Rev. Appl.* **10**, 064037 (2018).
- [19] W.-A. Li, G.-Y. Huang, J.-P. Chen, and Y. Chen, Nonreciprocal enhancement of optomechanical second-order sidebands in a spinning resonator, *Phys. Rev. A* **102**, 033526 (2020).
- [20] X. Zhang, C.-L. Zou, L. Jiang, and H. X. Tang, Cavity magnomechanics, *Sci. Adv.* **2**, e1501286 (2016).
- [21] J. Li, S.-Y. Zhu, and G. S. Agarwal, Magnon-photon-phonon entanglement in cavity magnomechanics, *Phys. Rev. Lett.* **121**, 203601 (2018).
- [22] Z.-X. Liu, B. Wang, H. Xiong, and Y. Wu, Magnon-induced high-order sideband generation, *Opt. Lett.* **43**, 3698 (2018).
- [23] C. A. Potts, E. Varga, V. A. S. V. Bittencourt, S. V. Kusminskiy, and J. P. Davis, Dynamical backaction magnomechanics, *Phys. Rev. X* **11**, 031053 (2021).
- [24] R.-C. Shen, J. Li, Z.-Y. Fan, Y.-P. Wang, and J. Q. You, Mechanical bistability in Kerr-modified cavity magnomechanics, *Phys. Rev. Lett.* **129**, 123601 (2022).

- [25] Z. Shen, G.-T. Xu, M. Zhang, Y.-L. Zhang, Y. Wang, C.-Z. Chai, C.-L. Zou, G.-C. Guo, and C.-H. Dong, Coherent Coupling between phonons, magnons, and photons, *Phys. Rev. Lett.* **129**, 243601 (2022).
- [26] D. Hatanaka, M. Asano, H. Okamoto, Y. Kunihashi, H. Sanada, and H. Yamaguchi, On-chip coherent transduction between magnons and acoustic phonons in cavity magnomechanics, *Phys. Rev. Appl.* **17**, 034024 (2022).
- [27] C. Kong, B. Wang, Z.-X. Liu, H. Xiong, and Y. Wu, Magnetically controllable slow light based on magnetostrictive forces, *Opt. Express* **27**, 5544 (2019).
- [28] S.-N. Huai, Y.-L. Liu, J. Zhang, L. Yang, and Y.-X. Liu, Enhanced sideband responses in a PT-symmetric-like cavity magnomechanical system, *Phys. Rev. A* **99**, 043803 (2019).
- [29] W. Zhang, D.-Y. Wang, C.-H. Bai, T. Wang, S. Zhang, and H.-F. Wang, Generation and transfer of squeezed states in a cavity magnomechanical system by two-tone microwave fields, *Opt. Express* **29**, 11773 (2021).
- [30] W. Qiu, X. Cheng, A. Chen, Y. Lan, and W. Nie, Controlling quantum coherence and entanglement in cavity magnomechanical systems, *Phys. Rev. A* **105**, 063718 (2022).
- [31] J. Li, Y.-P. Wang, J.-Q. You, and S.-Y. Zhu, Squeezing microwaves by magnetostriction, *Natl. Sci. Rev.* **10**, nwac247 (2022).
- [32] C. A. Potts, V. A. S. V. Bittencourt, S. Viola Kusminskiy, and J. P. Davis, Magnon-phonon quantum correlation thermometry, *Phys. Rev. Appl.* **13**, 064001 (2020).
- [33] H. Xiong, Magnonic frequency combs based on the resonantly enhanced magnetostrictive effect, *Fundam. Res.* **3**, 8 (2023).
- [34] Z.-X. Liu, J. Peng, and H. Xiong, Generation of magnonic frequency combs via a two-tone microwave drive, *Phys. Rev. A* **107**, 053708 (2023).
- [35] G.-T. Xu, M. Zhang, Y. Wang, Z. Shen, G.-C. Guo, and C.-H. Dong, Magnonic frequency comb in the magnomechanical resonator, *Phys. Rev. Lett.* **131**, 243601 (2023).
- [36] Z.-X. Liu, Dissipative coupling induced UWB magnonic frequency comb generation, *Appl. Phys. Lett.* **124**, 032403 (2024).
- [37] Z. X. Liu and H. Xiong, Ultra-slow spin waves propagation based on skyrmion breathing, *New. J. Phys.* **25**, 103052 (2023).
- [38] Z.-B. Yang, J.-S. Liu, A.-D. Zhu, H.-Y. Liu, and R.-C. Yang, Nonreciprocal transmission and nonreciprocal entanglement in a spinning microwave magnomechanical system, *Ann. Phys. (Berlin)* **532**, 2000196 (2020).
- [39] Y. Xu, J.-Y. Liu, W. Liu, and Y.-F. Xiao, Nonreciprocal phonon laser in a spinning microwave magnomechanical system, *Phys. Rev. A* **103**, 053501 (2021).
- [40] X. Wang, K.-W. Huang, and H. Xiong, Nonreciprocal sideband responses in a spinning microwave magnomechanical system, *Opt. Express* **31**, 5492 (2023).
- [41] B. Wang, X. Jia, D.-W. Zhang, C. Li, Y. Wang, and X.-H. Lu, Rotation-modulated higher-order sidebands spectra based on the Sagnac effect, *Appl. Phys. Express* **14**, 092001 (2021).
- [42] H. Zhang, X. Shang, Q. Liao, A. Chen, and W. Nie, Nonreciprocal quantum coherence in spinning magnomechanical systems, *Phys. Rev. A* **109**, 013719 (2024).
- [43] S. Chakraborty and C. Das, Nonreciprocal magnon-photon-phonon entanglement in cavity magnomechanics, *Phys. Rev. A* **108**, 063704 (2023).
- [44] Z.-Y. Wang, X.-W. He, X. Han, H.-F. Wang, and S. Zhang, Nonreciprocal PT-symmetric magnon laser in spinning cavity optomagnonics, *Opt. Express* **32**, 4987 (2024).
- [45] J. Chen, X.-G. Fan, W. Xiong, D. Wang, and L. Ye, Nonreciprocal photon-phonon entanglement in Kerr-modified spinning cavity magnomechanics, *Phys. Rev. A* **109**, 043512 (2024).
- [46] A. V. Chumak, Vasyuchka, and B. Hillebrands, Magnon spintronics, *Nat. Phys.* **11**, 453 (2015).
- [47] V. A. S. V. Bittencourt, C. A. Potts, Y. Huang, J. P. Davis, and S. Viola Kusminskiy, Magnomechanical backaction corrections due to coupling to higher order Walker modes and Kerr nonlinearities, *Phys. Rev. B* **107**, 144411 (2023).
- [48] C. A. Potts, Y. Huang, V. A. S. V. Bittencourt, S. Viola Kusminskiy, and J. P. Davis, Dynamical backaction evading magnomechanics, *Phys. Rev. B* **107**, L140405 (2023).
- [49] A. A. Serga, A. V. Chumak, and B. Hillebrands, YIG magnonics, *J. Phys. D* **43**, 264002 (2010).
- [50] C. A. Potts and J. P. Davis, Strong magnon-photon coupling within a tunable cryogenic microwave cavity, *Appl. Phys. Lett.* **116**, 263503 (2020).
- [51] M. Aspelmeyer, T. J. Kippenberg, and F. Marquardt, Cavity optomechanics, *Rev. Mod. Phys.* **86**, 1391 (2014).
- [52] C. W. Gardiner and P. Zoller, *Quantum Noise* (Springer, Berlin, 2000).
- [53] H. Xiong, L.-G. Si, X.-Y. Lü, X. Yang, and Y. Wu, Carrier-envelope phase-dependent effect of high-order sideband generation in ultrafast driven optomechanical system, *Opt. Lett.* **38**, 353 (2013).
- [54] Z.-X. Liu and Y.-Q. Li, Optomagnonic frequency combs, *Photonics Res.* **10**, 2786 (2022).
- [55] J. L. Krause, K. J. Schafer, and K. C. Kulander, High-order harmonic generation from atoms and ions in the high intensity regime, *Phys. Rev. Lett.* **68**, 3535 (1992).
- [56] J. J. Macklin, J. D. Kmetec, and C. L. Gordon, III, High-order harmonic generation using intense femtosecond pulses, *Phys. Rev. Lett.* **70**, 766 (1993).
- [57] N. Bloembergen, From nanosecond to femtosecond science, *Rev. Mod. Phys.* **71**, S283 (1999).
- [58] P. Del'Haye, A. Schliesser, O. Arcizet, T. Wilken, R. Holzwarth, and T. J. Kippenberg, Optical frequency comb generation from a monolithic microresonator, *Nature (London)* **450**, 1214 (2007).
- [59] T. J. Kippenberg, R. Holzwarth, and S. A. Diddams, Microresonator-based optical frequency combs, *Science* **332**, 555 (2011).
- [60] A. Metelmann and A. A. Clerk, Nonreciprocal photon transmission and amplification via reservoir engineering, *Phys. Rev. X* **5**, 021025 (2015).
- [61] D. L. Sounas and A. Alù, Non-reciprocal photonics based on time modulation, *Nat. Photonics* **11**, 774 (2017).
- [62] F. Lecocq, L. Ranzani, G. A. Peterson, K. Cicak, R. W. Simmonds, J. D. Teufel, and J. Aumentado, Nonreciprocal microwave signal processing with a field-programmable Josephson amplifier, *Phys. Rev. Appl.* **7**, 024028 (2017).
- [63] Y. Wang, D. Zhu, Y. Yang, K. Lee, R. Mishra, G. Go, S. Oh, D. Kim, K. Cai, E. Liu, S. D. Pollard, S. Shi, J. Lee, K. L. Teo, Y. Wu, K.-J. Lee, and H. Yang, Magnetization switching by magnon-mediated spin torque through an antiferromagnetic insulator, *Science* **366**, 1125 (2019).

- [64] J. Han, P. Zhang, and J. T. Hou, Mutual control of coherent spin waves and magnetic domain walls in a magnonic device, *Science* **366**, 1121 (2019).
- [65] M. Song, I. Iorsh, P. Kapitanova, E. Nenasheva, and P. Belov, Wireless power transfer based on magnetic quadrupole coupling in dielectric resonators, *Appl. Phys. Lett.* **108**, 023902 (2016).
- [66] Y. Arita, M. Mazilu, and K. Dholakia, Laser-induced rotation and cooling of a trapped microgyroscope in vacuum, *Nat. Commun.* **4**, 2374 (2013).
- [67] R. Reimann, M. Doderer, E. Hebestreit, R. Diehl, M. Frimmer, D. Windey, F. Tebbenjohanns, and L. Novotny, GHz rotation of an optically trapped nanoparticle in vacuum, *Phys. Rev. Lett.* **121**, 033602 (2018).
- [68] J. Ahn, Z. Xu, J. Bang, Y.-H. Deng, T. M. Hoang, Q. Han, R.-M. Ma, and T. Li, Optically levitated nanodumbbell torsion balance and GHz nanomechanical rotor, *Phys. Rev. Lett.* **121**, 033603 (2018).